PROCEEDINGS, Thirty-Eighth Workshop on Geothermal Reservoir Engineering
Stanford University, Stanford, California, February 11-13, 2013
SGP-TR-198

APPLICATION OF NEUTRON IMAGING TO INVESTIGATE FLOW THROUGH FRACTURES FOR EGS

Yarom Polsky, Lawrence M. Anovitz, Philip Bingham and Justin Carmichael

Oak Ridge National Laboratory
1 Bethel Valley Rd
Oak Ridge, TN, 37831 U.S.A
e-mail: polskyy@ornl.gov

ABSTRACT

There is an ongoing effort at Oak Ridge National Laboratory to develop a unique experimental capability for investigating flow through porous and fractured media using neutron imaging techniques. This capability is expected to support numerous areas of investigation associated with flow processes relevant to EGS including, but not limited to: experimental visualization and measurement of velocity profiles and other flow characteristics to better inform reduced-order modeling of flow through fractures; laboratory scale validation of flow models and simulators; and a 'real-time' tool for studying geochemical rock/fluid interactions by noninvasively measuring material effects such as precipitation and dissolution in EGS-representative conditions.

Demonstrating the ability of the technique to generate useful quantitative data is the primary focus at this stage of the effort. Details of the experimental setup and neutron imaging technique will be discussed in this communication, including the description of a custom designed, high pressure, neutron scattering and imaging compatible triaxial flow cell.

INTRODUCTION

The ability to describe, quantify and manage fluid flow through porous and fractured geological media is of great importance to all sub-surface hydrological applications including geothermal energy extraction. The ability to accurately simulate flow through fractures is of particular importance to EGS as it will likely be the basis for designing optimal EGS field configurations. With relatively little field experience from which to build an understanding of best practice, simulation will help inform many critical well field design considerations including optimal well trajectories, fracture characteristics, preferred fracture distribution and control/management of fluid injection and production.

The quantification of flow through fractures has a rich history of investigation involving a multitude of modeling and experimental approaches. Standard flow through fracture models are based on idealizations such as plane Poiseuille flow. Early investigations of fluid flow through fractures often focused on validating the so called cubic law derived from the Poiseuille model [Witherspoon *et al.*, 1980]. Parallel and subsequent efforts sought to develop effective or statistical representation of the geometrical variations that are invariably present in geological fractures to capture features not accounted for in the cubic law model including aperture changes and surface roughness [e.g. Snow, 1965, Neuzil *et al.*, 1981; Browm, S.R.,1987, Waite *et al.*, 1999 and Dicman *et al.* 2004].

These studies often combined experimental work with the theoretical analysis as a validation component. Flow quantification was generally performed using bulk fluid mass/volume flow measurements as is typical for permeometry. However, while bulk flow measurements are useful for validating the integrated effects predicted by phenomenological models of fluid flow, they fail to capture details such as flow fields that also underpin these models and can be used to ascertain their credibility.

More detailed experimental characterizations of flow have focused on studying two-phase mixtures, for which it is easier to construct experiments in which visual data can be collected to corroborate models. These efforts typically employ light based camera systems to image flows through transparent flow boundaries [Fourar *et al.*, 1995 and Chen *et al.*, 2004]. These techniques have proven very useful for studying flow structure and comparing the accuracy

of different relative permeability models but are not applicable to actual geological media.

Other techniques for investigating material structure and flow within geological materials include X-ray radiography and diffraction, NMR and, less commonly, neutron radiography and diffraction [Mees *et al.,* 2003, Jasti *et al.,* (1992), Fukushima, 1999 and Deinart *et al.,* 2002]. These techniques have the advantages of being able to resolve internal structural details of geological specimens using non-destructive means and in many ways are complementary to each other.

Neutron scattering and attenuation-based techniques have many distinctive advantages over other radiographic imaging methods for studying certain types of physical processes such as fluid flow because cold and thermal neutrons are more highly attenuated by materials with large hydrogen compositions while they more easily penetrate higher Z materials such as those used in structural applications. Experiments exploiting this behavior may therefore be devised to study flow behaviors in samples even when thick pressure vessel walls and large sample masses are present. The use of X-rays and NMR in these applications is typically inadequate due to penetration depth limitations and magnetic field distortions, respectively.

The objective of this project is to develop an experimental setup and methodology for subjecting EGS-representative core samples with artificial or natural fractures and fracture features to a triaxial stress state at EGS-representative temperatures (up to 350°C) and pumping high pressure fluid through the sample while imaging and measuring fluid flow characteristics using high-flux neutron beams. Towards this end, a geothermal pressure test cell and flow system has been developed that can accommodate 38.1 mm diameter, 152.4 mm long core samples and apply a radial confining pressure up to 10,000 psi with fluid flow pressures up to 5,000 psi. This cell has been specially designed to optimize the transmission of neutrons and permit improved imaging of the interior of the sample of interest.

Proof-of-principle measurements of the system have been performed and will be discussed in this paper. Results from three types of experiments using a granite core sample will be presented: imaging of the water/air flow front through an initially air filled fracture; imaging of the H_2O/D_2O or borated H_2O/D_2O flow front for a continuous flow experiment using D_2O as a pulsed contrast agent; and measurement of the precipitation of boric acid on the fracture surface after pumping water saturated with boric acid through the sample. Techniques for injecting fluid contrast agents to permit visualization and quantification of flow profiles are also being developed and will be described along with future development plans.

EXPERIMENAL SETUP

Geothermal Pressure Cell

The centerpiece of the experimental setup is a custom designed pressure cell capable of holding core samples with a diameter of 38.1 mm and length of up to 152.4 mm (Figure 1). Samples are placed inside a thin Kapton sleeve that fits over the stem pieces at the ends of the vessel through which fluid is injected or discharged. A compression cylinder and seal ring are used to seal the inner and outer surfaces of the sleeve against the stem piece and inner wall of the pressure vessel respectively. This sealing arrangement permits pressurization of the annular space between the sleeve and pressure vessel wall through a tapped through hole on the outside of the vessel. The pressure applied in this space compresses the sleeve producing a confining pressure that acts on the sample's radial face. The seal on the opposite face of the sleeve permits independent pressurization of the axial face of the sample through the stem piece thus producing a triaxial stress state.

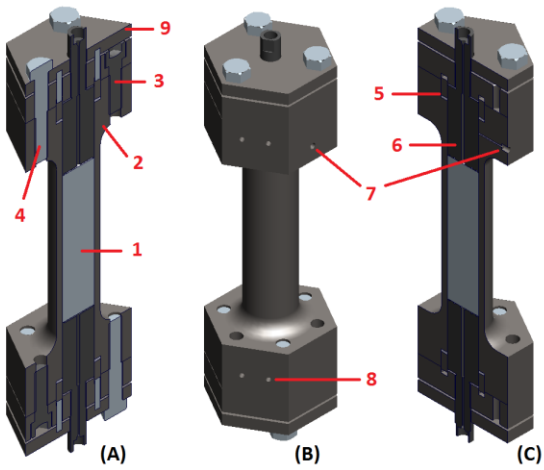

Figure 1 - The geothermal fluid flow cell. An isometric view of the cell is shown in (B), while (A) and (C) are both cross-sectional views. View (A) shows the internal fasteners which bear the load of the internal pressure. Labels: (1) core sample, (2) vessel body, (3) internal retaining fasteners, (4) seal forming fasteners, (5) seal area, (6) fluid flow stem, (7) liner pressure port, (8) mounting holes, and (9) seal forming plate assembly.

Operating specifications for the cell are:

- Max confining/radial pressure – 10,000 psi
- Max axial/flow pressure – 5,000 psi
- Max temperature – 350°C

The titanium cell body and Kapton sleeve are relatively transparent to neutrons to mitigate scattering effects that may adversely influence radiographic or diffraction measurements. They also have low activation cross-sections enabling the cell to be handled, reloaded, transported and reused immediately after neutron irradiation experiments because induced radioactivity is minimal. A neutron radiograph of a sandstone sample inside the cell is shown below in Figure 2. The end stem piece is removed and a plastic tie wrap is instead inserted into the assembly for reference and contrast. Note that the thickness of the Kapton sleeve is clearly discernible in the image.

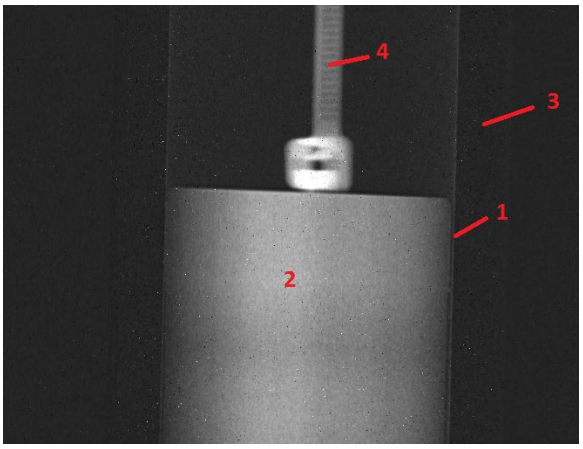

Figure 2 – Neutron radiograph of sandstone sample within pressure cell without end stem piece and zip tie inserted for reference. Labels: (1) Kapton sleeve, (2) Sandstone core, (3) Cell wall, (4) zip tie

Flow Circuit

A schematic of the fluid pressurization circuit is shown below in Figure 3. Annular pressurization to produce sample confining pressure is accomplished either using a gas bottle, for pressures up to 2,500 psi, or an air operated gas booster pump, for pressures up to 10,000 psi. Nitrogen gas is typically used as the pressurization fluid as it is generally readily available and does not affect neutron measurements.

The system currently has two options for sample fluid injection depending on the needed flow rates. Experiments requiring very low rates on the order of 100 mL/min, such as flow through intact porous media, utilize a syringe style high pressure pump. Flow through samples with engineered or natural fractures require considerably higher fluid injection rates to represent geothermally-meaningful conditions. Maximum target flow rates are specified based on the assumption that it will be useful to have the ability to investigate flow through samples up to the laminar to turbulent transition region. The transition occurs at Reynolds numbers greater than 1400 for flow through parallel plates, the idealized model for a smooth fracture. This results in a desirable maximum fluid flow rate on the order of 3 L/min. The system is currently equipped with a 5,000 psi triplex pump with a maximum flow rating of 17 L/min. A back pressure valve is used to control the discharge pressure downstream of the pressure cell and is the means for controlling the pressure of the fluid pumped through the sample.

Both pumping systems are connected via either high pressure hose or capillary tubing so they can be located outside the neutron beam line instrument cave for easy access during experiments. Heating of the fluid lines and pressure cell to achieve geothermally relevant temperatures is typically accomplished using heater tape and insulation wrap. The pressure cell can alternatively be heated using induction heating. It may also prove to be necessary in the future to inductively heat a fluid accumulator for extended time high flow rate experiments.

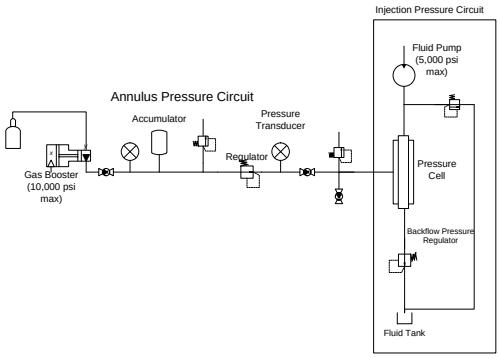

Figure 3: Geothermal pressure cell process and instrumentation diagram

EXPERIMENTAL DESCRIPTIONS

Three different types of experiments were performed at the NIST BT-2 imaging beam line. Two of the experiments were designed to verify the ability of neutron imaging to measure moving fluid interfaces while the third experiment evaluated the ability of the technique to quantify fracture wall deposits produced during a precipitation experiment.

All tests were performed using a 38.1 mm diameter by 152.4 mm long Westerly granite sample with an engineered fracture. The fracture was created by cutting the core through the center in the axial direction to produce two half-cylinders. The two sections were then glued back together using two 3.18 mm wide by 1.6 mm high by 152.4 mm long aluminum spacers at the outer edges to offset the granite faces. The sandwiched assembly produced a 31.75 mm wide by 1.6 mm high channel through which fluid could flow.

Gas/Liquid Interface Experiments

The first set of experiments were intended to verify the ability of neutron imaging to capture details associated with the flow boundary of a moving air/water interface through a sample installed in the geothermal pressure vessel. The experiment was initiated with only air present in the engineered fracture and images were captured as water was injected through the cell. As a proof-of-concept, this simple experiment was necessary because neutron sources have fluences that are typically many orders of magnitude below those of X-ray and light sources. The ability to obtain sufficient neutron counts from which to generate an image over a short time period through the titanium pressure cell and rock sample was therefore in question.

The primary objectives of this experiment were to: 1) determine the minimum exposure time needed to image the flow interface; and 2) determine the amount of flow structure detail that could be resolved. Rapid exposure times are also needed in this application to reduce distortion of the image caused by the moving front. For example, for a flow front moving at 3 m/s, the front itself moves 3 mm during an exposure time of 1 ms limiting the resolution of the imaging system beyond purely optical considerations.

Liquid/Liquid Interface Experiments

The second set of experiments was intended to determine if liquids with substantially different neutron absorption and scattering cross-sections could be used as contrast agents to image flow structure of continuous liquid flow through the vessel. The assumption underlying this approach is that the injection of slugs of a liquid with significantly different contrast compared to the initial circulation fluid, but with similar fluid flow properties, permits imaging of the velocity profile of the fluid moving through the fracture. For example, if the flow follows a Poiseuille idealization and the velocity at the center is sufficiently high, then the shape of the moving interface of the initial circulating fluid and contrast fluid should resemble the Poiseuille parabolic profile if mixing of the fluids is minimal.

The two liquids were injected into the system in different manners depending on the pumping arrangement utilized. For the low flow rate experiments, the outputs of two separate pumps were teed together and a control system was used to turn off output from one pump and turn on the other in order to inject contrast agent. Only one pump was available for the high flow rate experiments so injection of contrast agent was accomplished by using solenoid valves on a manifold tied to the pump suction to switch between fluids.

Discernment of detail in this experiment is dependent on the selection of liquids with suitable contrast, exposure time considerations as evaluated in the first set of experiments, and minimal mixing of the fluids. Water has a relatively high total cross section for both thermal and cold neutrons resulting in high attenuation of the neutron beam through the sample. Heavy water, or D_2O, has a total cross section that is on the order of 1/10 that of water for thermal neutrons. It was hoped that this contrast would be adequate for viewing fluid structure details. Borated water (water saturated with boric acid) was also used in some experiments. Earlier static experiments have shown that borated H_2O has a 15% greater cross section than H_2O to provide even greater contrast.

Precipitation Experiments

The last set of experiments aimed to determine if quantitative measurement of precipitate deposition on the rock face could be made by imaging the contents of the pressure cell. It is envisioned that this experimental capability can be used in the future to provide quantitatively meaningful and unique information that can be used to validate geochemical interaction models.

This experiment was designed to produce rapid precipitation of a high contrast substance to ensure that significant amounts of material could deposit on the granite faces and be measured in the limited experimental time available. Borated water was heated to a temperature of roughly 70°C in an accumulator vessel with excess solid boric acid and forced through the system. The capillary lines between the accumulator and geothermal pressure cell were heated to a temperature higher than that of the accumulator to mitigate precipitation of boric acid in the injection lines. The pressure cell was maintained at a temperature of roughly 50°C to permit precipitation of the boric acid on the granite faces within the vessel as fluid was injected.

Imaging Setup Used at NIST

The neutron imaging facility at the NIST reactor is positioned at Beam Tube 2 (BT-2), and the main application for the development of this facility has been the study of fuel cells. As shown in 4, the neutron beam has a direct view of the reactor through a number of collimators, filters, and apertures. For the experiments performed in this effort, the aperture was set at the maximum size available in their current configuration to produce the maximum number of neutrons for the shortest exposure time. The aperture settings resulted in an open aperture of 1.5 cm which produces a neutron fluence rate of 1.4×10^7 neutrons/cm^2/s. Neutron imaging facilities typically set up their system to produce as parallel a beam as possible and then place the object (7 in **Error! Reference source not found.**) as close as possible to the detector (8 in **Error! Reference source not found.**) to prevent a loss in resolution due to penumbra (blurring caused by the source size). With the 1.5 cm aperture, the resulting L/D of the system is 400. Placing the pressure chamber as close as possible to the camera positioned the center of our rock core approximately 5cm from the surface of the imaging detector resulting in minimal blurring due to penumbra effects.

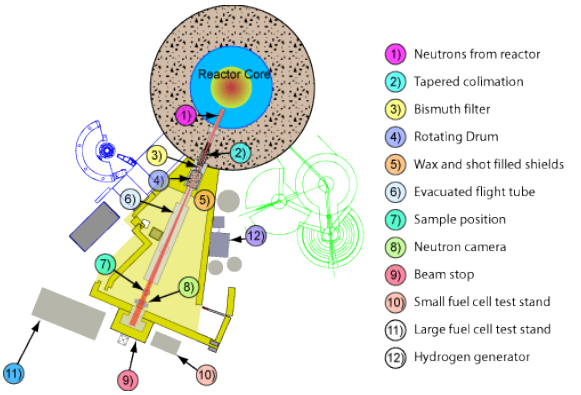

Figure 4: Design of the neutron imaging facility at NIST. (http://physics.nist.gov/MajResFac/NIF/facility.html)

A scintillator based imaging detector was used for the experiment consisting of a 100µm thick lithium fluoride based scintillator plate to convert neutrons to photons, followed by a turning mirror, a focusing lens to image the scintillator and an Andor scientific CMOS camera. This lens and camera were set such that a single pixel in the image covered a 48.5 x 48.5 µm area on the scintillator. Blurring in the scintillator limits resolution for the imaged object to 100µm, so the camera is sampling slightly better than the Nyquist sampling rate to provide 100µm resolution neutron images of the rocks. The sCMOS camera has the capability of high speed image acquisition with low noise. Overall exposure time required is a function of the neutron fluence rate, scintillator thickness, imaging lens aperture, and quantum efficiency of the camera. During the experiment, testing was performed at several exposure times and binning levels on the camera. To stop motion for the highest speed flow fronts, we selected a 10ms exposure time with 3x3 binning of image pixels (300um resolution). Computed tomographic (CT) imaging was also to study precipitation within the rock. Since we were not trying to capture dynamic motion, the CT data was collected with 1sec exposure times with 1x1 binning for improved SNR and 100um resolution.

EXPERIMENTAL RESULTS

The ensuing discussion of results for all experiments is primarily qualitative. Attention is focused on whether or not the acquired data supports the use of the neutron imaging techniques as a means of investigating flow structure and, in the case of the precipitation experiment, quantification of chemical interaction effects.

Gas/Liquid Interface Results

Images of the gas/liquid interface were successfully acquired for both low flow rate and high flow rate experiments. The progression of the interface in a series of 10 ms images is shown below in Figure 5 for the high flow rate experiments (a flow rate of approximately 1 L/min was used). Water is represented by the bright region of the image. An air bubble is seen rising through the moving water and breaking the surface in this series. The shape of the water/air interface is also clearly discernible and to some extent measureable.

3x3 binning has been used on the camera to capture these images, so pixels within these images are 145.5µm square in size for a resolution of approximately 300µm. There are 190 of these pixels across the water flowing through the crack. With this current setup, the grainy texture of the images clearly indicates a fairly low signal to noise ratio. The last row in Figure 5 shows the overlay of an edge extraction performed on the second image in each of the top two rows containing the image sequence. This extraction consisted of a noise filter followed by a threshold to obtain a binary image. Finally an edge filtering step was performed on the binary image and overlayed on the original image. From this we see that the general edge shape is clear, but the noise does cause roughness of the edges. A rough estimate of edge resolution based on this intial edge extraction

effort would be 10 pixels (1.45mm). Based on results from this first proof-of -principle, efforts to improve neutron flux and capture are planned to increase the signal to noise ratio in future tests. Possible steps are use of a thicker scintillator to trade resolution for improve neutron capture efficiency, shifting detection system toward reactor to trade field of view for increased neutron flux, and trading resolution for noise by further pixel binning on the detector.

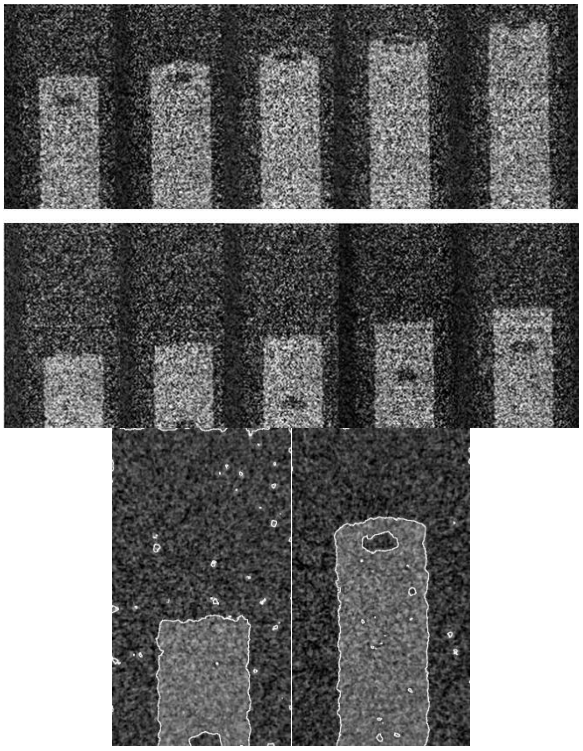

Figure 5: Air/Water interface images for fast flow with visible air bubble (water is brighter image component). Lower two images show edge extraction of second images in each of top two rows.

It is believed that some of the interface irregularities seen in the images are a result of the manner in which fluid flow is supplied from the pressure vessel stem piece to the fracture entrance. The current design of the stem piece preferentially supplies the center of the crack, potentially leading to jetting effects for the high flow rate experiment. Management of flow entering the sample will be further discussed in the liquid/liquid interface experimental results.

Interface detail for images taken using longer exposure times for low flow rate experiments (30 mL/ minute) is much more distinct and consistent in progressive images. Figure 6 below shows a subset of interface close-ups taken for low flow rate experiments using a 100 ms exposure time. It is therefore believed that if adequate contrast is present and fluid delivery can be properly controlled, this technique shows great promise for resolving the detail necessary for flow simulation comparison.

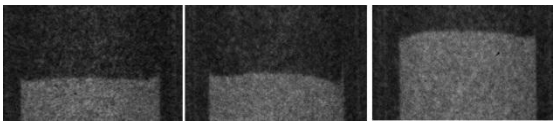

Figure 6: Air/Water interface images with visible air bubble (water is brighter image component).

Liquid/Liquid Interface Results

Pulsed contrast experiments using either H_2O or borated H_2O and D_2O were completed with mixed success. Figure 7 below shows D_2O injection into a fracture initially filled with Borated H_2O at 30 mL per minute flow rates using 20 ms exposure times. The displacement of the borated H_2O is clearly visible, however, there is no clearly recognizable front. This is likely due to diffusive mixing of the fluids as they are slowly pumped through the system.

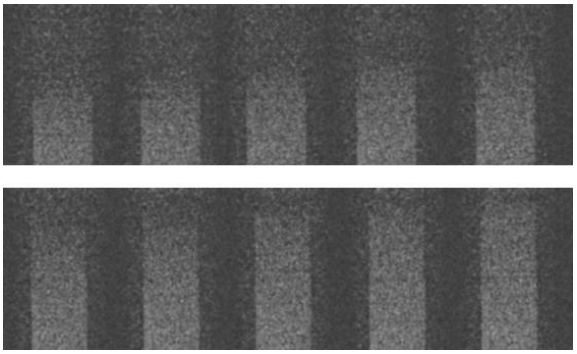

Figure 7: D_2O /H_2O interface images for slow flow (H_2O is brighter image component).

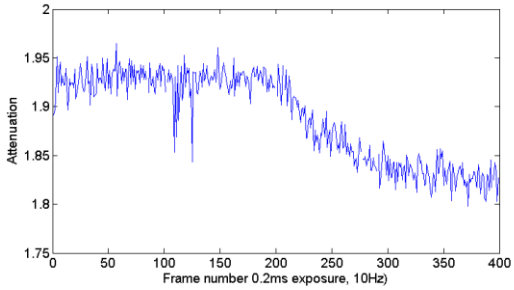

Figure 8: Attenuation averages within a control volume for low flow rate pulsed contrast experiment.

This smearing of the front is further evidenced in the plot of average neutron count attenuation within a

control volume (evaluated over a fixed area in the radiograph) versus frame number (Figure 8). The transition from high attenuation to low attenuation takes roughly 100 frames at a 10 Hz capture rate (10 seconds) clearly indicating that a sharp front is not present. The change is nonetheless visible in the images and measureable in the processed data.

High flow rate experiments performed with sequential injection of contrast liquids were less compelling by comparison. This is evident in the average attenuation versus frame rate plot below in Figure 9. There is a noticeable variation of the measured attenuation as flow transitions between D_2O and H_2O. However, the smooth and gradual transition of the curve from higher to lower attenuation averages implies that there is no definitive flow front. Such a front would typically resemble a step change in measured intensity. The event identified near the beginning of the plot, for example, is an example of a rapid and drastic intensity reduction caused by an air bubble advancing through the measured control volume.

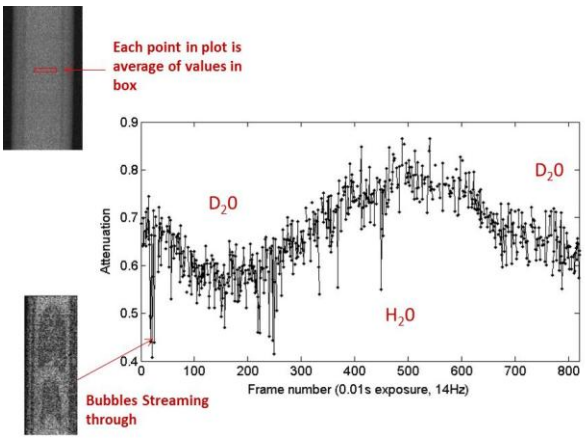

Figure 9: Attenuation averages within a control volume for high flow rate pulsed contrast experiment.

The gradual indication of intensity variation between contrast pulses is also a result of mixing of H2O and D2O. Diffusive mixing may occur at any point in the system and is likely the dominant mixing mechanism for the low flow rate experiments. For the high flow rate setup, the manner in which fluids are introduced at the pump and distributed through the pressure cell are more likely to have contributed to forced mixing of the fluids. In the case of fluid introduction, switching fluid types at the pump suction results in a combination of fluids residing in the pump body for a limited period of time until the pump body volume is completely exchanged. Some mixing will occur in most pump types at this stage by virtue of the flow patterns caused by pumping action and valve cycling. The pump utilized for the experiment is of the triplex plunger variety further compounding mixing issues because the source of forcing pressure applied to the fluid varies in location depending on the three plunger locations during the pumping cycle.

The stem piece through which fluid is injected into the pressure cell is likely another cause of mixing issues. It currently consists of a 6.35 mm hole through located on center along with a series of radial and circumferential channels cut into the face that abuts the sample face. The channels are intended to distribute flow across the core face but it is likely that for the high flow rate experiments flow is preferentially directed towards the center of the fracture producing a jet-like effect.

Precipitation Results

Continuous fluid injection for the precipitation experiment was unsuccessful because of precipitation within and nearly complete occlusion of the tubing between the accumulator and the pressure cell. Boric acid nonetheless precipitated on the granite faces and neutron images were captured showing deposition details. Figure 10 shows a neutron radiograph through the cell and a post-test photo of the sample face with consistent deposition locations.

Computed tomograph data sets of the cell were captured before and after the experiment by rotating the cell within the imaging system. CT reconstruction of the post deposition provided three-dimensional representations of the depositions in the rock crack. Figure 11 shows rendered images of the deposit (with the rock and cell material removed) looking perpendicular to the rock face, at 45 degrees to the rock face and parallel to the rock face. With 1second exposures showing excellent signal to noise as seen by the radiograph in Figure 10, the reconstructed data has a resolution of approximately 100µm which permits detailed three dimensional quantification of the deposit structure.

While it is acknowledged that the precipitate in this case is a high contrast material, it is believed that such studies performed in the future with materials more representative of geothermal conditions can still be resolved with adequate detail to support non-invasive geochemical interaction studies. The addition of minor amounts of materials with high neutron cross sections may be incorporated into reactive mixtures in some instances to increase contrast and improve deposition quantification. Filling of the fracture volume with water, D_2O or

another liquid can alternatively be used to identify the extent of deposits as the deposits will form the boundary of the fluid (this approach may not be feasible with high permeability samples).

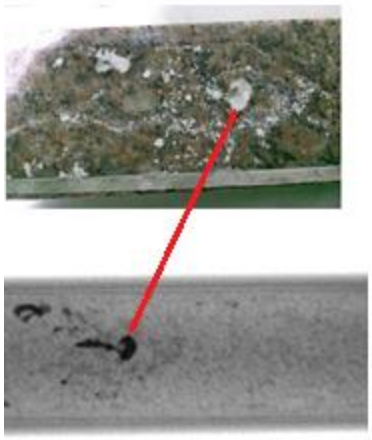

Figure 10: Post-test sample photo and prior neutron radiograph through cell.

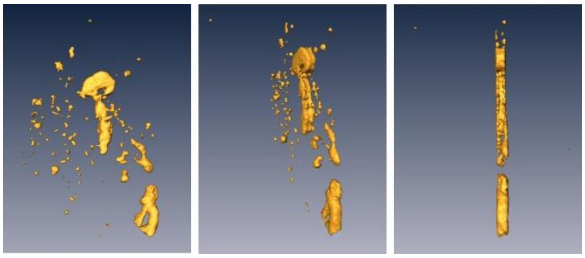

Figure 11: CT of the boric acid deposition within engineered fracture at angles of 0 degrees, 45 degrees and 90 degrees relative to face normal.

The results acquired in these experiments imply that this technique is immediately applicable to perform relevant geochemical studies and can be performed in a variety of different modes. If the deposition rate of the experiment is relatively short, real-time flow radiographs can be taken with periodic flow interruptions for detailed CT reconstructions. Experiments involving slow deposition rates can be executed in any suitable location over the required interaction time and then brought to the beam line for measurements.

CONCLUSIONS

It is believed that the proof-of-principle experiments performed demonstrate the potential for neutron imaging to be used as a tool for quantitatively and qualitatively describing the structure of flow moving through a fracture. In the case where high contrast fluids are present, and minimal mixing occurs, such as for a distinct liquid/gas interface, it has been demonstrated that relatively high fidelity flow structure details can be resolved from the acquired images even with 10 ms exposure times.

This is not currently the case for experiments involving liquid/liquid interfaces where it was demonstrated that mixing of the primary fluid and contrast agent is likely occurring. There was also not a great amount of contrast between the fluid types used for these experiments. Future efforts in flow structure imaging will focus on three primary goals: 1) Modifying the experimental setup by designing an improved contrast fluid injection arrangement and optimizing other flow transition regions, such as the pressure cell flow stem/rock interface, to mitigate mixing; 2) Selecting fluid sets with greater contrast to improve image clarity (this will have to be done in a manner that considers how variation of fluid properties will affect interface structure); and 3) Refining beam line optics, data acquisition and image processing techniques where possible to improve image quality and reduce exposure times.

Finally, the ability to measure three-dimensional structure of precipitation deposits on rock faces within a pressure cell at high resolution was demonstrated. It is believed that this technique can be immediately used to perform measurements for experiments aimed at modeling and quantifying rock/fluid chemical interactions.

ACKNOWLEDGMENT

Research supported by the Geothermal Technologies Office, Office of Energy Efficiency and Renewable Energy, U.S. Department of Energy under contract DE-AC05-00OR22725, Oak Ridge National Laboratory, managed and operated by UT-Battelle, LLC.

We also acknowledge the support of the National Institute of Standards and Technology, U. S. Department of Commerce, in providing the neutron research facilities used in this work.

REFERENCES

Brown, S.R. (1987), "Fluid Flow Through Rock Joints: The Effect of Surface Roughness", *Journal of Geophysical Research*, **92**, pp. 1,337 – 1,347.

Chen C.Y., Horne, R.N. and Fourar, M. (2004), "Experimental Study of Liquid-Gas Flow Structure

Effects on Relative Permeabilities in a Fracture" *Water Resources Research*, **40**, W08301.

Deinart, M.R., Parlange, J.Y., Steenhuis, T., Throop, J., Unlu, K. and Cady, K.B. (2002), "Measurement of Fluid Contents and Wetting Front Profiles by Real-Time Neutron Radiography", *Journal of Hydrology*, **290 (3-4)**, pp. 192-201.

Dicman, A., Putra, E. and Schechter, D.S. (2004), "Modeling Fluid Flow Through Single Fratures Using Experimental, Stochastic and Simulation Approaches", *SPE 89442*.

Fourar, M., and S. Bories (1995), "Experimental Study of Air-Water Two Phase Flow Through a Fracture (Narrow Channel)", *Int. J. Multiphase Flow*, **21**, pp. 621– 637.

Fukushima, E., "Nuclear Magnetic Resonance as a Tool to Study Flow" (1999), *Annu. Rev. Fluid Mech.*, **31**, pp. 95-123.

Jasti, J.K. and Fogler, H.S. (1992), "Application of Neutron Radiography to Image Flow Phenomena in Porous Media", *AIChE Journal*, **28 (4)**, pp.481 – 488.

Klimczak, C., Schultz, R.A., Parashar, R. and Reeves, D.M. (2010), "Cubic Law with Aperture-Length Correlation: Implications for Network Scale Fluid Flow", *Hydrogeology Journal*, **18 (4)**, pp. 851-862.

Mees, F., Swennen, .R., Van Geet, M. and Jacobs, P. (2003), "Applications of X-Ray Computed Tomography in the Geosciences", *Geological Society, London, Special Publications*, **215**, p. 1-6.

Neuzil, C.E. and Tracy, J.V. (1981), "Flow Through Fractures", *Water Resources Research*, **17**, pp. 191-199.

Snow, D.T. (1965) "A Parallel Plate Model of fractured permeable Media", PhD Thesis Univ. of Calif., Berkeley.

Waite, M.E., Ge, S. and Spetzler, H. (1999), "A New Conceptual Model for Fluid Flow in Discrete Fractures: An Experimental and Numerical Study", *Journal of Geophysical Research*, **104**, pp. 13,049 – 13,059.

Witherspoon, P.A., Wang, J.S.Y., Iwai, K. and Gale, J.E. (1980),"Validity of Cubic Law for Fluid Flow in a Deformable Fracture", *Water Resources Research*, **16**, pp. 1016-1024.